KERNFORSCHUNGSZENTRUM

KARLSRUHE

September 1969

KFK 1069

Institut für Angewandte Kernphysik

A Method for Neutron Resonance Spin Assignment by Differential Scattering Analysis

G.J. Kirouac, J. Nebe

GESELLSCHAFT FÜR KERNFORSCHUNG M.B.H.

KARLSRUHE

KERNFORSCHUNGSZENTRUM KARLSRUHE

September 1969 KFK 1069

Institut für Angewandte Kernphysik

A Method for Neutron Resonance Spin Assignment by Differential Scattering Analysis

by

George J. Kirouac and Jürgen Nebe

Gesellschaft für Kernforschung m.b.H., Karlsruhe

Abstract

This work is intended as an exploratory investigation of the use of few-angle neutron scattering measurements to assign resonance spins and parities. The cross section shape as a function of the scattering angle is illustrated for s,p and d-wave neutrons.
Text book examples are calculated for isolated resonances and for interfering resonances. A specific example is given for ^{40}Ca and a scattering experiment which is in preparation is outlined. It is concluded that study of the resonance shape observed at a few scattering angles can be used profitably to assign spins and parities even for closely spaced interfering resonances.

Diese Arbeit stellt eine Studie für ein Neutronenstreuexperiment dar, durch das Spins und Paritäten von Resonanzen bestimmt werden können. Die Form der Anregungsfunktionen in Abhängigkeit des Streuwinkels wird für s-, p- und d-Wellen erläutert. Für isolierte und interferierende Resonanzen werden Anschauungsbeispiele gegeben. Ein spezielles Beispiel wird für ^{40}Ca gerechnet und ein entsprechendes Streuexperiment, das in Vorbereitung ist, umrissen. Diese Arbeit zeigt, daß die Untersuchung der Resonanzformen bei einigen wenigen Winkeln vorteilhaft zur Bestimmung von Spins und Paritäten sogar eng benachbarter, interferierender Resonanzen eingesetzt werden kann.

TABLE OF CONTENTS :

I. Introduction

For the development of nuclear theory and models it is important to determine the quantum numbers of excited states of the compound nucleus, especially the total angular momentum and parity. Neutron spectroscopy has long been one of the popular experimental methods. In addition to the direct application of these data to fast reactor calculations, questions of a more fundamental nature such as the J and l dependence of resonance spacings and strength functions depend upon the determination of spin parameters. The following will briefly present some of the principal methods for obtaining such data from neutron measurements.

The magnitude of the total angular momentum is frequently available from total neutron cross section data. Under conditions of high resolution, the spin weighting factor g, equal to $(2J+1)/2(2I+1)$ can be calculated from the observed $\sigma_{max}-\sigma_{min}$. Thus the J value can be determined. When the s-wave potential scattering is large, s-wave resonances can be identified from an asymmetry in the resonance shape due to interference between the resonance and the potential scattering. In other cases an incorrect assignment can be prevented by showing that the sum rule for neutron widths[1] is violated. This technique is applied by dividing the observed resonance width by the penetration factor associated with the assumed partial wave. The resulting reduced neutron width γ_n^2 may not exceed the estimated width of a single particle state.

The most unambiguous method used for spin and parity assignment involves transmission measurements with polarized neutron beams or samples. However, the necessary degree of polarization is difficult to obtain for broad energy regions. This necessitates laborious measurements of small changes in the transmission for the polarized and unpolarized system.

Still other techniques have used the capture γ-ray emission spectrum to assign the parity of compound states. The spin and parity of the initial state can be found if the spin and parity are known for the low-lying final state and the nature of the transition is known. This method is not unambiguous since it depends on the inherent weakness of certain types of transitions (e.g. magnetic dipole transitions are usually favored over electric dipole and higher order multipole transitions are unfavored.) A difficulty arises because even those transitions of known multipolarity can show large fluctuations in strength from different initial states. The unscrambling of various transitions requires extensive analysis of the data.

A powerful remaining method of analysing experimental data for spin determination is based on the nuclear dispersion theory formalism, such as that developed by Wigner and Eisenbud[2]. The data consists of differential cross sections measured at different angles for a number of closely spaced neutron bombarding energies in the vicinity of a resonance. Because of the angular dependence of the cross sections expressed in Legendre polynomials a set of properly chosen angles allows a unique determination of the l-value of a level by the shape of the cross section curves. The choice of the spin parameters can easily be accomplished for different resonances at the angles chosen in the experiment. (The general appearance of these standard shapes does not change markedly with energy or with choice of hard-sphere phase shifts.)

This method has been used successfully in light nuclei[3-11] although in those instances it was mostly applied to relate the results of phase shift analysis to independently derived level parameters. The main reasons for the limitation of this method to light nuclei are due to the difficulties of obtaining intense neutron sources, efficient neutron detectors and acceptable energy resolution. When these problems are overcome, partial wave assignment will clarify ambiguities as it did in a recent experiment[12].

Here the angular dependence of interference effects in the scattering cross section was measured to determine the l-value of the 1.15 keV resonance in ^{56}Fe.

In this report the theory of differential neutron scattering using the R-matrix formalism is briefly reviewed. The method of spin and parity determination by few angle scattering measurements is discussed at length and many illustrative examples are given. A specific example for $^{40}Ca(n,n)$ is shown and a simple scattering experiment is proposed.

II. Review of Theory

The problem of calculating the angular dependence of scattering and reaction processes for nuclear particles has been worked out by some authors in great detail[13,14]. The following section will outline the development one may follow for the particular problem at hand, i.e. the assignment of the angular momentum and parity of the compound state by neutron scattering. This introduction is intended to provide a logical foundation for the scattering formulae used in the analysis of data and a definition of the terms used. The development follows that of Blatt and Biedenharn[14].

The formalism begins with the definition of an amplitude $q_{\alpha s/u;\alpha' s'/u'}$. This represents a transition amplitude for the reaction process $\alpha s/u \rightarrow \alpha' s'/u'$ in which an incident plane wave with a specified two body partition α, channel spin s and projection $/u$ is observed after the reaction as a plane wave in direction $\Omega_{\alpha'}$, with partition α', channel spin s' and projection $/u'$. The primed quantities need not be different from the unprimed ones. In the case of elastic neutron scattering for example $\alpha = \alpha'$. Denoting the two nuclei by X_α and Y_α

we can define the following channel parameters

$$M_\alpha = \frac{M_{X_\alpha} \cdot M_{Y_\alpha}}{M_{X_\alpha} + M_{Y_\alpha}} \quad , \qquad \text{the reduced mass for partition } \alpha$$

$$\vec{r}_\alpha = \vec{r}_{X_\alpha} - \vec{r}_{Y_\alpha} \quad , \qquad \text{the relative coordinate}$$

$$E_\alpha \quad , \qquad \text{the energy of relative motion between } X_\alpha \text{ and } Y_\alpha$$

$$k_\alpha = \frac{1}{\lambda\!\!\!^{-}_\alpha} = \left(\frac{2ME}{\hbar^2}\right)^{1/2} \quad , \qquad \text{the wave number}$$

$$v_\alpha = \frac{\hbar k_\alpha}{M_\alpha} \quad , \qquad \text{the relative velocity}$$

$$\Omega_\alpha, \ \theta_\alpha \phi_\alpha \quad , \qquad \text{the solid angle in direction } \vec{r}_\alpha \text{ and the polar angles.}$$

For this two-body partition α the generalized incoming and outgoing waves are given by

$$J_{\alpha lm} = \frac{i^l Y_l^m(\Omega_\alpha)\, I_{\alpha l}}{r_\alpha v_\alpha^{1/2}} \qquad \sigma_{\alpha lm} = \frac{i^l Y_l^m(\Omega_\alpha)\, O_{\alpha l}}{r_\alpha v_\alpha^{1/2}}$$

where $I_{\alpha l}$ and $O_{\alpha l}$ are the solutions of the free-particle radial equation and Y_l^m is the normalized spherical harmonic. The channel is completely specified by the quantum numbers $c = (\alpha l s m/u)$ and wave functions

$$\mathcal{I}_c = \mathcal{I}_{\alpha l m} \chi_{\alpha s/u} \qquad \mathcal{O}_c = \mathcal{O}_{\alpha l m} \chi_{\alpha s/u}$$

where $\chi_{\alpha s/u}$ is the wave function of nuclei X_α and Y_α combined to yield angular momentum $\vec{s} = \vec{J}_{X_\alpha} + \vec{J}_{Y_\alpha}$ with z-component $/u$.

A linear combination of $\mathcal{I}_c$ and $\mathcal{O}_c$ constitutes the most general wave function in the external region which satisfies the wave equation for energy E_α

$$\Psi_{E_\alpha} = \sum_{cc'} (\mathcal{I}_c \delta_{cc'} - U_{cc'} \mathcal{O}_{c'}) A_c \qquad (1)$$

where the amplitudes of the incoming waves A_c are arbitrary. The quantity $U_{cc'}$ is the collision matrix[16] and represents the probability amplitude for a collision from channel c into channel c'. For reactions with only one open channel (e.g. pure elastic scattering), U may be related to a phase shift δ by $U = \exp(2i\delta)$. In general, for N open channels U is an N-by-N matrix which is unitary and symmetric.

In the usual development, the next step requires the expansion of the incoming plane wave as partial waves in the spherical harmonics. An incident beam of uncharged particles with unit flux is written as

$$\Psi^{\alpha s/u}_{\text{inc.}} = \frac{e^{ik_\alpha z_\alpha}}{\sqrt{v_\alpha}} \chi_{\alpha s/u} = \frac{i\sqrt{\pi}}{k_\alpha} \sum_l (2l+1)^{1/2} (\mathcal{I}_{\alpha lo} - \mathcal{O}_{\alpha lo}) \chi_{\alpha s/u} \qquad (2)$$

where $\chi_{\alpha s/u}$ is the previously introduced channel wave function. In this expansion m=0 has been assumed since the different spin orientations are incoherent and we are concerned only with unpolarized beams. By comparing (2) with the total wave function given in (1), the amplitudes of the incoming spherical waves are given as

$$A_c = i\sqrt{\pi}\ \lambda_\alpha\ (2l+1)^{1/2}\ \delta_{mo}$$

for the channel $c = (\alpha, l, s, m=0, /u)$.
Then the total wave function is

$$\psi_{E_\alpha} = \psi^{\alpha s/u}_{inc.} + i\sqrt{\pi}\ \lambda_\alpha^2 \sum_{lc'} (2l+1)^{1/2}\ \delta_{mo} \left[J_c\ \delta_{cc'} - U_{cc'}\ \sigma_{c'} \right]$$

$$- i\sqrt{\pi}\ \lambda_\alpha^2 \sum_{l} (2l+1)^{1/2} \left[J_{\alpha lo} - \sigma_{\alpha lo} \right] \chi_{\alpha s/u}$$

This is the wave function of a state with unit flux incident in channel $\alpha s/u$ and various outgoing waves. The outgoing wave in channel $\alpha' s'/u'$ is

$$\psi^{\alpha' s'/u'}_{out} = \frac{i\sqrt{\pi}}{k_\alpha} \sum_{ll'm'} (2l+1)^{1/2} \left[\delta_{\alpha\alpha'}\ \delta_{ss'}\ \delta_{ll'}\ \delta_{/u/u'}\ \delta_{m'o} - \right.$$

$$\left. - U_{\alpha l s o/u;\ \alpha' l' s' m'/u'} \right] \sigma_{c'}$$

$$= \frac{i}{r_{\alpha'} k_\alpha} \sum_{ll'm'} \sqrt{\frac{\pi v_\alpha}{v_{\alpha'}}}\ i^{l-l'}\ (2l+1)^{1/2} \left[\delta_{\alpha\alpha'} \delta_{ss'} \delta_{ll'} \delta_{/u/u'} \delta_{m'o} - \right.$$

$$\left. - U_{\alpha l s o/u;\ \alpha' l' s' m'/u'} \right] Y^{m'}_{l'}\ O_{\alpha' l'}$$

Now, the amplitude of the scattered wave is identified as,

$$q_{\alpha s/u;\ \alpha' s'/u'}(\Omega_{\alpha'}) = i\sqrt{\pi}\,\lambda_{\alpha} \sum_{ll'm'} (2l+1)^{1/2} \cdot \left[\delta_{\alpha\alpha'}\,\delta_{ss'}\,\delta_{ll'}\,\delta_{/u/u'}\,\delta_{mo} - U_{\alpha ls0/u;\ \alpha' l' s' m'/u'}\right] Y_{l'}^{m'}(\Omega_{\alpha'}) \tag{3}$$

and the differential cross section is simply given by,

$$d\sigma_{\alpha s/u;\ \alpha' s'/u'} / d\Omega = \left| q_{\alpha s/u;\ \alpha' s'/u'}(\Omega_{\alpha'}) \right|^2 \tag{4}$$

If the beam of incident particles is unpolarized and we do not separately observe the spins s' or their projections /u' in the outgoing channels we need to average equation (4) over incident channels with s, /u and to sum over outgoing channels s', /u'. This is most easily done by making use of the total angular momentum quantum number J. Thus, the scattering matrix U^J with elements $U^J_{\alpha sl,\alpha' s' l'}$ is introduced. The relationship of U^J and U involves the vector addition coefficients connecting the states $\alpha lsJM$ and $\alpha lsm/u$

$$U_{\alpha lso/u;\ \alpha' l' s' m'/u'} = \sum_{JM} (lso/u \mid JM)\,(l's'm'/u' \mid JM)\,U^J_{\alpha sl;\alpha' s' l'}$$

Following the method of Blatt and Biedenharn[14] symmetry considerations show that the actual evaluation of the differential

cross section formula

$$d\sigma_{\alpha\alpha'} = \frac{1}{2s+1} \sum_{\mu=-s}^{s} \sum_{\mu'=-s'}^{s'} d\sigma_{\alpha s\mu;\ \alpha' s'\mu'}$$

can be simplified considerably. This can be reduced to an expression involving no sums over magnetic quantum numbers. The necessary development is due to Racah[15]. The final result can be written most simply in termsof the so called Z coefficients $\bar{Z}(l_1 J_1 l_2 J_2 | sL)$ defined as

$$\bar{Z}(l_1 J_1 l_2 J_2 | sL) = i^{L-l_1+l_2} (2l_1+1)^{1/2} (2l_2+1)^{1/2} (2J_1+1)^{1/2} (2J_2+1)^{1/2}$$

$$W(l_1 J_1 l_2 J_2 | sL) \cdot (l_1 l_2 00 | L0)$$

where W is a Racah coefficient[15] and $(l_1 l_2 00|L0)$ are the usual vector addition coefficients. The differential cross section is then given by the well known Biedenharn formula,

$$d\sigma_{\alpha s;\alpha' s'} = \frac{\lambda_\alpha^2}{2s+1} \sum_{L=0} B_L(\alpha,s;\ \alpha' s')\ P_L(\cos\Theta)\ d\Omega \qquad (5)$$

where

$$B_L(\alpha s;\alpha' s') = \frac{(-)^{s-s'}}{4} \Sigma\, \bar{Z}(l_1 J_1 l_2 J_2 | sL)\, \bar{Z}(l_1' J_1 l_2' J_2 | sL) \cdot$$

$$\mathrm{Re}\{(\delta_{\alpha\alpha'}\, \delta_{ss'}\, \delta_{l_1 l_1'} - U^{J_1\pi_1}_{\alpha l_1 s;\alpha' l_1' s'}) \cdot (\delta_{\alpha\alpha'}\, \delta_{ss'}\, \delta_{l_2 l_2'} - U^{J_2\pi_2}_{\alpha l_2 s;\alpha' l_2' s'})\}$$

The sum runs over $J_1\pi_1 J_2\pi_2 l_1 l_1' l_2 l_2'$ and all sums are unrestricted going from 0 to ∞ . In practice, only one of these is really infinite. The other five sums are finite because of selection rules, associated with parity conservation.

Up to this point general expressions for reaction cross sections have been obtained in terms of the collision matrix U. This matrix hides all of the real physics of the problem. Practical applications of the theory must now deal specifically with the collision matrix. Several methods are in general use; we will consider only the R-matrix theory of Wigner. The basic idea of the theory is to describe the cross section (i.e. the collision matrix) in terms of eigenfunctions and eigenvalues defined close to the surface of the nucleus. Eigenfunctions of the internal region are then related to the well-known wavefunctions of the external (potential-free) region via the logarithmic derivative at the channel radius. This idea is common to other reaction theories such as the method of Kapur and Peierls, but the Wigner theory has the advantage of real eigenvalues and energy independent parameters. In this theory the U matrix is simply related to the R-matrix[16] by simple functions defined in the external region

$$U = \Omega\, P^{1/2} \cdot \underline{/1-R(L-B)/}^{-1}\, \underline{/1-R(L^*-B)/} \cdot P^{-1/2}\, \Omega$$

where Ω, L and P are diagonal matrices defined in terms of the external wavefunctions. Elements of the R-matrix in turn are completely defined in terms of the two energy independent parameters E_λ and $\gamma^2_{\lambda c}$

$$R_{cc'} = \sum_\lambda \frac{\gamma_{\lambda c}\gamma_{\lambda c'}}{E_\lambda - E}$$

The usual difficulty with the Wigner theory lies in the inversion of the matrix $\underline{/1-R\ (L-B)/}$ which becomes difficult for the case of several open channels. This difficulty has been avoided in the Kapur Peierls method at the expenses of the use of energy dependent parameters analogous to $\gamma^2_{\lambda c}$ and E_λ. In our present case we deal with a single open channel (the elastic reaction channel) and the R-matrix becomes a simple function.

III. Predictions of the Theory

In the previous section, a general outline of the theory of the differential neutron scattering cross section was presented. One of the useful applications of the theory is to light or closed shell nuclei where only the elastic scattering channel needs to be explicitly treated. This situation occurs for most of the fast neutron analysis performed to date.

A Fortran programm[+] has been written to calculate the differential scattering cross section as a function of neutron energy and angle. Multi-level effects have been included. At present, only zero spin ground state nuclei can be treated, but the calculation can be easily generalized.

[+] The program input consists of an arbitrary set of resonances with assumed spins and parities. The program provides an output list of the calculated cross sections and a Calcomp picture of the resonance shape (energy dependence) at various laboratory scattering angles.

The first of the results presented in this section illustrates the characteristic resonance shapes versus scattering angles which occur for isolated s, p and d-wave resonances. All calculations were performed for a resonance at 0.9 MeV, with width 30. keV and hard sphere radius 5. fermi. However, these parameters are not of primary importance as long as the s-wave phase shift dominates p and d-wave. Figures 1-5 show the shape of isolated s, p and d-wave resonances at five laboratory scattering angles (44.0°, 58.8°, 88.6°, 124.2° and 149.3°). Certain symmetries are apparent. The s-wave resonance has qualitatively the same shape at all scattering angles. The dominant resonance and interference parts of the cross section are contributed by the L=0 term in the Legendre expansion (eqn. 5) and therefore are independent of the angle. A smaller contribution comes from the interference between s-wave resonance and p-wave potential scattering via the L=1 term. This behaves as cos θ and causes a noticeable increase in the off-resonance scattering at forward angles and a decrease at back angles.

The p-wave resonances have a strong forward-backward scattering asymmetry about 90° where the interference term changes sign. This is due to the interference between p-wave resonance scattering and s-wave potential which manifests itself through the L=1 term (cos θ) of the expansion. At forward angles, the interference is destructive below resonance and constructive above. At back angles, the effect is reversed. These differences in the shape of s and p-wave resonances at forward and backward scattering angles permit their identification in the scattering cross section. For example, a measurement of the scattered neutron energy spectrum at only two angles could be used to assign the spin state. We note that the characteristic behaviour of s and p-wave resonances is precisely reversed at high energies ($E_n \sim 10$ MeV) where the p-wave phase shift dominates s-waves. Now the p-wave resonance shape depends largely on the L=0 term and shows little angular dependence. At these

energies the s-wave resonance becomes asymmetric about 90° due to the dominant L=1 term.

The shape of the d-wave resonances is slightly more complicated. Here the strongest angular dependence occurs via the L=2 term from coherence between d-wave resonance and s-wave potential scattering. This term behaves as $3\cos^2\theta-1$ and the interference reverses sign at 54.7° and 125.3° in the C.M. system. At these angles, the coherence is zero and the resonance has purely Lorentzian shape. The direct resonance scattering comes from L=0 and L=2. The latter term reaches a maximum at 0° and 180° and has symmetry about a minimum at 90°.

In principle, s, p and d-wave resonances can be identified by a three angle scattering measurement. The limiting case of multiple-angle measurements corresponds to the standard phase shift analysis experiment.

The second set of examples of resonance shapes presented here concerns the coherent effects which occur in the differential scattering cross section between resonances of different spins and parities. For the total scattering cross section, the square of the scattering amplitude can be reduced to the real part of the collision matrix. The total scattering matrix then contains only diagonal elements with $l_1=l_2$ and $J_1=J_2$. Thus, in the total cross section, interference can occur only between resonances with the same spin and parity. The differential scattering cross section, however, depends on a collision matrix composed of diagonal elements as well as all possible cross product terms between levels. The Legendre expansion (eqn. 5) is only an equivalent form for the square of a sum of angular dependent scattering amplitudes (eqn. 3,4). If the differential cross section is integrated to obtain the total scattering, all terms except L=0 integrate to zero, and this term can only contain

elements with $l_1=l_2$ and $J_1=J_2$.

Figures 6-9 illustrate coherence in the differential scattering cross section for several combination of resonances with different spins and parities. For demonstration, interference between $1/2^+$-$1/2^-$, $1/2^+$-$3/2^+$, $1/2^-$-$3/2^-$ and $1/2^-$-$3/2^+$ resonances have been chosen. The coherent effects can be seen by comparison with the single level shapes and especially with the total scattering cross section. The figures also show the changing shape of the cross section as a narrow resonance is moved across a broad resonance.

The figures illustrate several examples in which resonance shapes change dramatically as levels move closer and the coherence becomes stronger. It is not the intention of this section to discuss all of these effects. The important point is that the coherent interactions follow directly from the theory and can be readily calculated. Our purpose here is merely to present a series of text book examples which can be referred to later.

The final examples deal with multi-level effects between resonances with the same spin and parity. These are shown in figures 10-14 for s, p and d-wave resonances. The figures also show the effect of moving a narrow resonance across a broad resonance. This demonstration is the counterpart in the differential cross section of the text book examples computed by Bowman et al.[17] for the multi-level interference in the total scattering cross section.

IV. An Example for ^{40}Ca

Up to this point, the theory has been briefly dicussed and several examples have been shown. We now offer an illustrative example for the application of the method to the determination of resonance spins and parities in ^{41}Ca. The total cross section of ^{40}Ca has previously been measured by several workers[17,18]. A recent analysis[19] of high resolution data has indicated that several large resonances in the energy range .8-1.0 MeV which were previously assigned to s-wave neutrons are better fitted by assuming p-waves. If the fit is forced with s-waves, an unrealistically small channel radius results.

We have calculated the shape of the ^{40}Ca differential scattering cross section for neutron energies .8-1.0 MeV. Energies and widths for the major resonances have been taken from total cross section analysis. New high resolution data[18] also show many narrow p and d-wave resonances, but these have not been included in the calculation. Figures 15-17 show the predicted shape of the cross section at three angles. Each figure corresponds to a different set of assumptions for the level spins and parities. Table I summarizes the assumptions. Careful examination of the figures indicates that it should be possible to determine if the broad resonances at 867, 886, 973 and 1009 keV are caused by s or p-wave neutrons. Even this complicated case containing closely spaced levels demonstrates the same features which occur for isolated resonances. The example of ^{40}Ca contains both coherent and multi-level interference.

V. A Proposed Scattering Experiment

The angular dependence of resonance line shapes can be used to unambiguously assign the spin and parity of levels of the

compound nucleus. We have shown that certain features and symmetries are characteristic of s, p and d-wave resonances. Knowledge of these features and especially our ability to precalculate the resonance shapes as a function of scattering angle leads us to propose that this method may be applied to determine spins and parities for possibly a large number of resonances. Asami and Moxon[12] have recently shown that the method is easily applied to an isolated resonance. We suggest that the method can also be used in the energy region where levels overlap and multilevel effects occur. To this end, we have outlined below a trial experiment for three scattering angles.

The Karlsruhe isochronous cyclotron has been used routinely for total cross section measurements. The time-of-flight spectrometer at this installation could also be used to perform few-angle scattering measurements. A three angle measurement for ^{40}Ca is currently in preparation. Calculations of the expected count rate indicate that with the present 20 KHz pulsing system, the sample to detector distance should be less than about 25 cm. The ^{40}Ca sample will be in the form of a right circular cylinder with its symmetry axis perpendicular to the neutron beam. This geometry assures uniform neutron attenuation at all scattering angles. The incident neutron beam will be collimated to a 7 cm x 14 cm size at 50 m. The scattering sample must necessarily be somewhat thick (.05-.1 atoms/barn) to achieve a favourable counting rate. Data from three scattering angles and a beam monitor will be simultaneously accumulated in an on-line computer. The 8 region data program (sample in and sample out) required for this measurement is in preparation.

It is important to note that this type of experiment has as its primary objective the measurement of the shape of neutron

resonances at various scattering angles. Thus, absolute differential scattering cross sections need not be obtained. Absolute detector efficiencies and the absolute incident neutron intensity are not required. Functions which vary slowly with the neutron energy, such as the incident flux shape and the energy dependent detector efficiency, are also of secondary importance. High angular resolution is not required and can be sacrificed to improve counting rates.

For ^{40}Ca, the total cross section has previously been measured and resonance energies and widths are generally known. Thus, the expected differential cross section can be precalculated for several sets of assumed level spins and parities as shown in figures 15-17. These precalculations also permit the optimal scattering angles to be chosen and the effects of multiple scattering can be visualized before the measurements are made.

VI. Summary

This paper is intended as an exploratory investigation of the use of a few-angle scattering measurement to assign resonance spins and parities. The general theory of differential scattering cross section has been presented briefly. We have calculated many text book examples showing the shape of the cross section as a function of scattering angle. The figures show isolated resonances as well as coherent effects between resonances. A specific example was illustrated for resonances in ^{40}Ca. Finally, we have briefly sketched a possible scattering experiment to utilize the method.

Multiple-angle scattering experiments have been used routinely for phase shift analysis of generally smooth cross sections.

Thus far, the method has been applied to resonance scattering only for the case of an isolated resonance. On the basis of the present study, we suggest that the method will also be useful for the case of closely spaced interfering resonances, even in the presence of multi-level effects.

Legend for Figures

□ Differential Cross Section (barns/steradian) $45.0^{\circ}_{C.M.}$

◇ Differential Cross Section (barns/steradian) $54.7^{\circ}_{C.M.}$

\+ Differential Cross Section (barns/steradian) $90.0^{\circ}_{C.M.}$

X Differential Cross Section (barns/steradian) $125.3^{\circ}_{C.M.}$

⧓ Differential Cross Section (barns/steradian) $150.0^{\circ}_{C.M.}$

⋈ Total Scattering Cross Section (barns) / 7.5

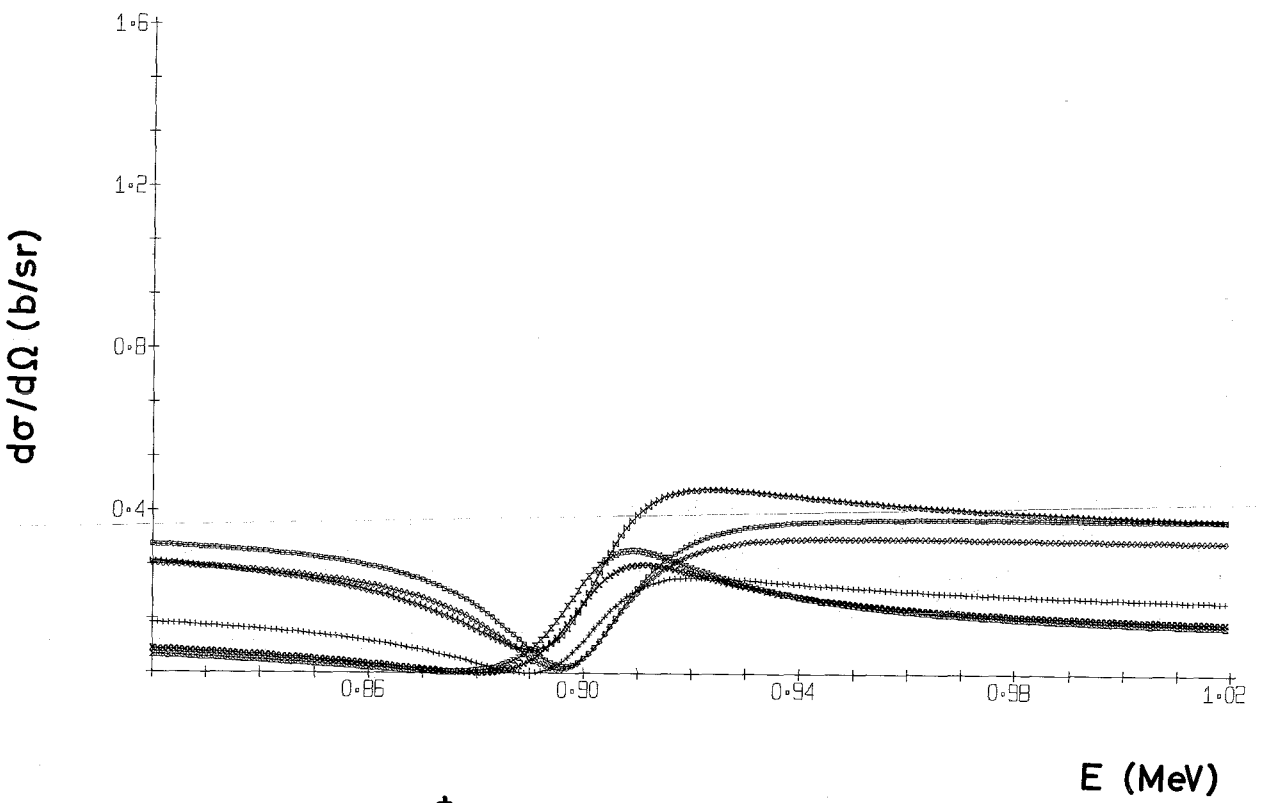

Fig. 1 Single $1/2^{+}$ Resonance

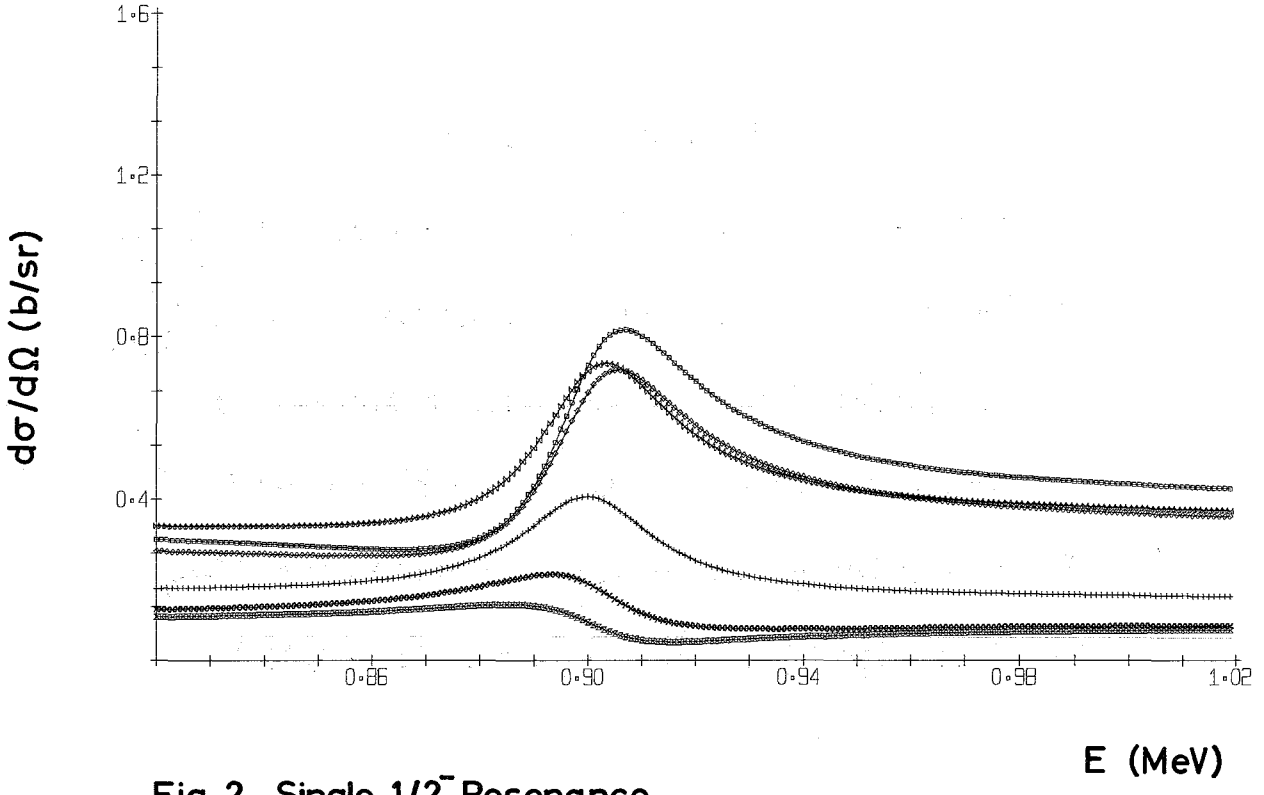

Fig. 2 Single $1/2^-$ Resonance

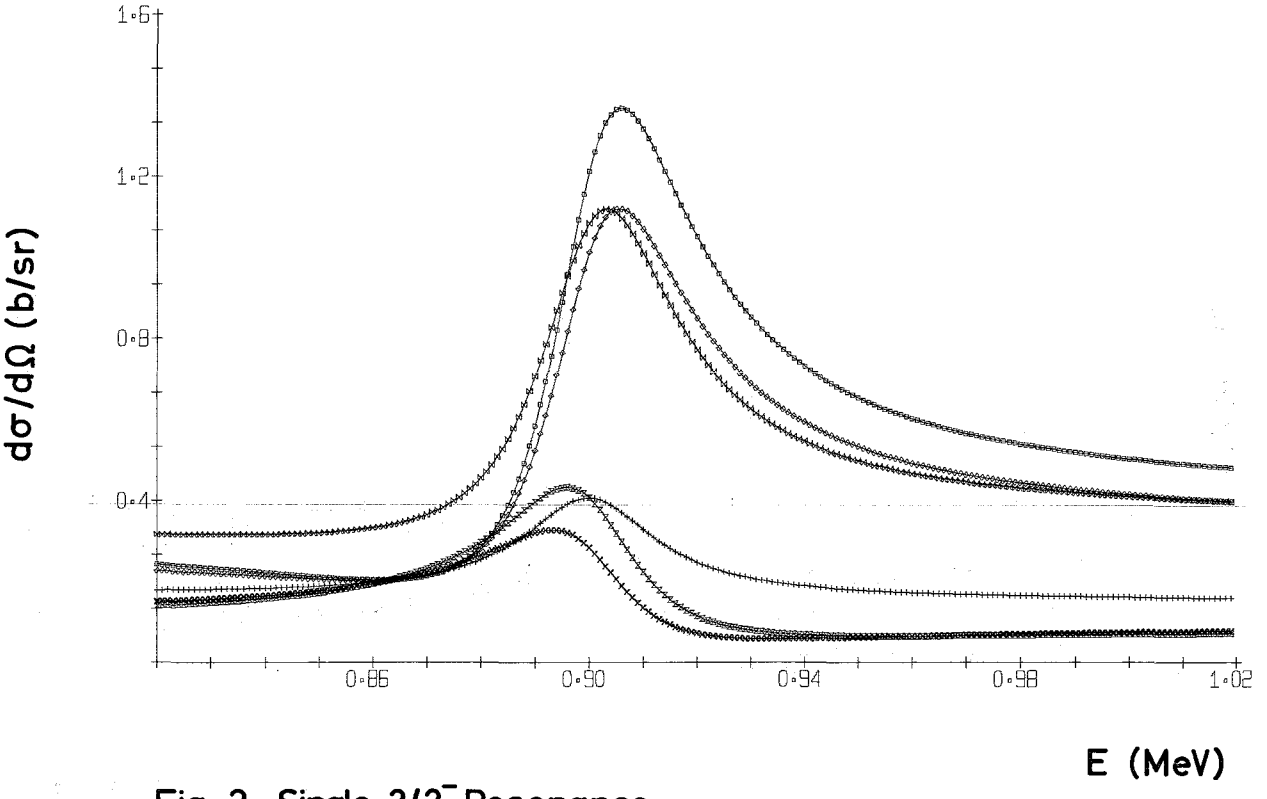

Fig. 3 Single $3/2^-$ Resonance

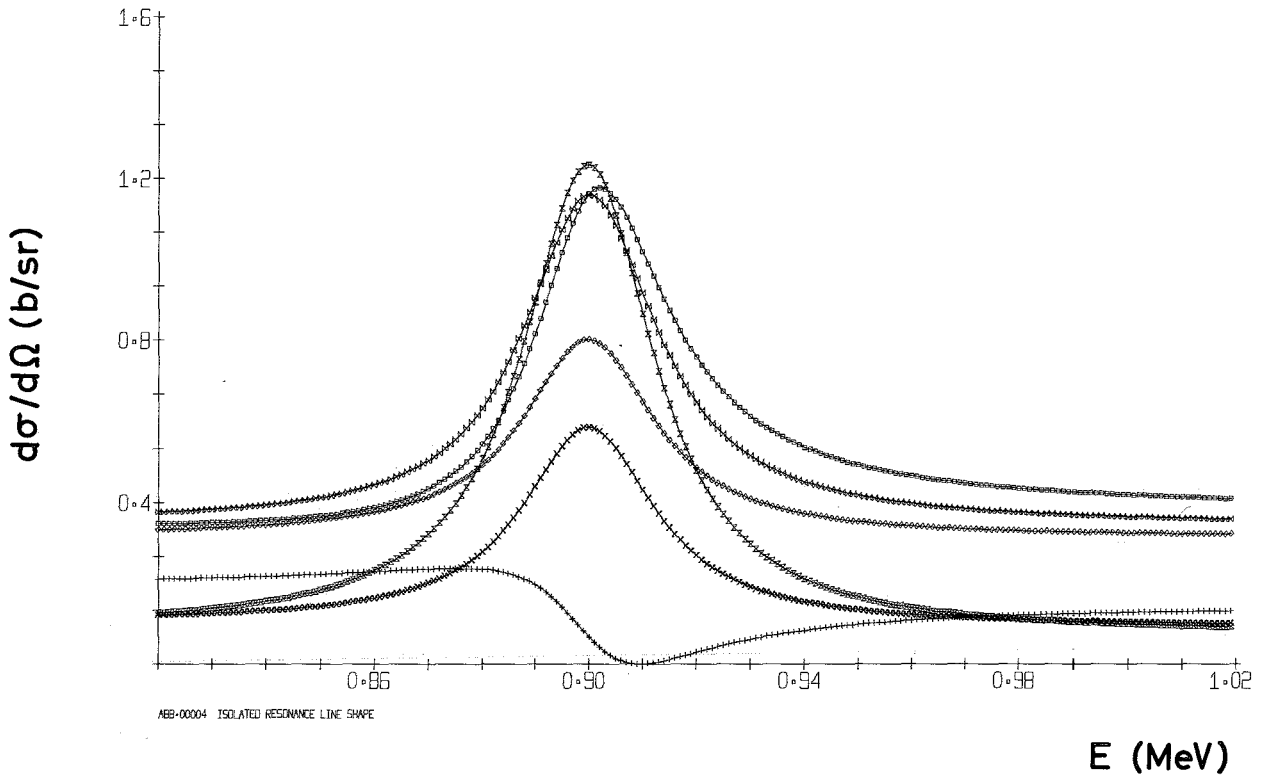

Fig. 4 Single $3/2^+$ Resonance

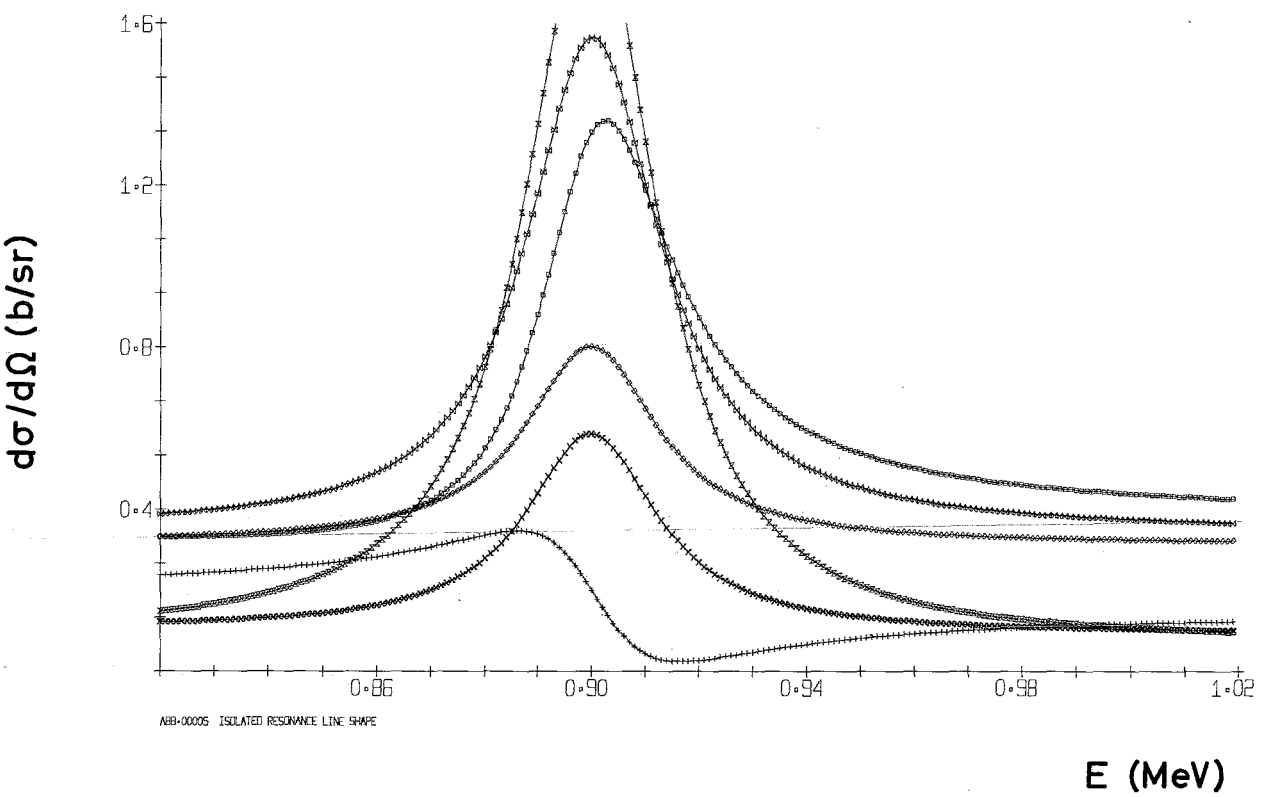

Fig. 5 Single $5/2^+$ Resonance

Differential Cross Sections (barns/steradian)

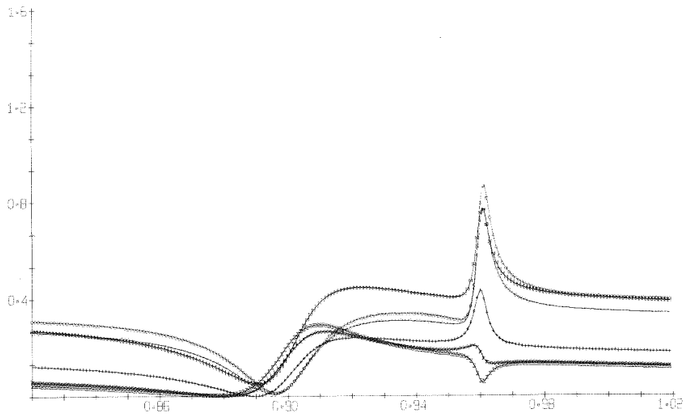
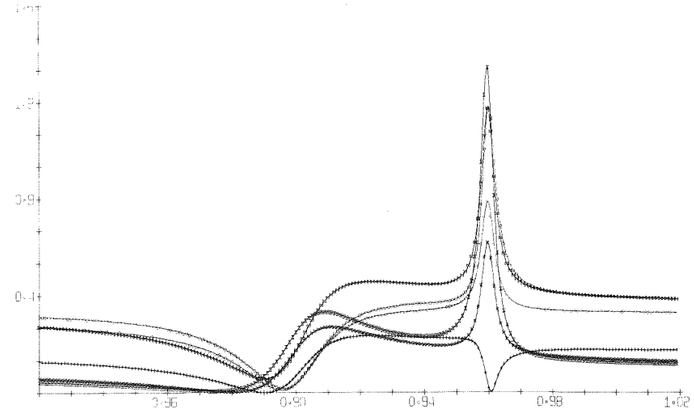
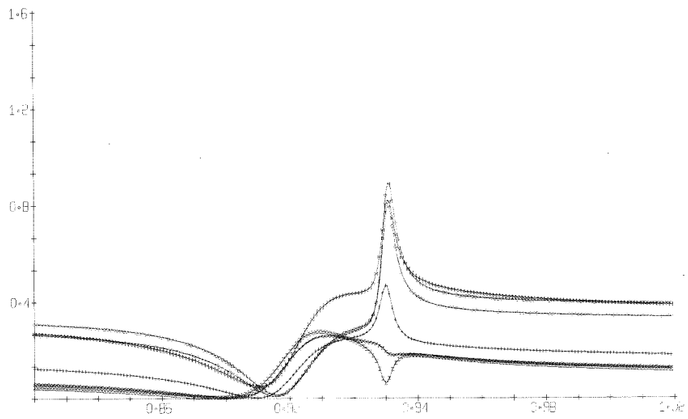
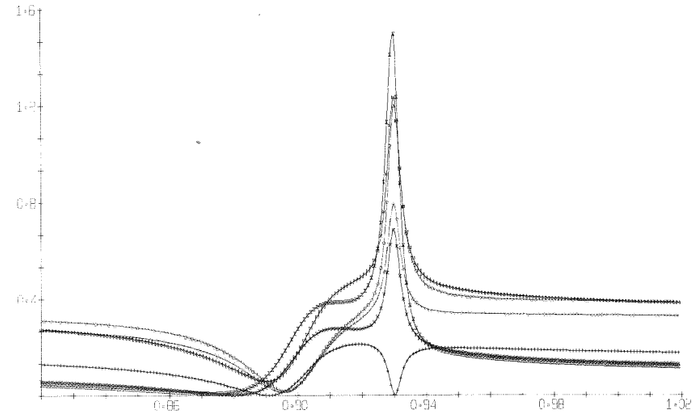
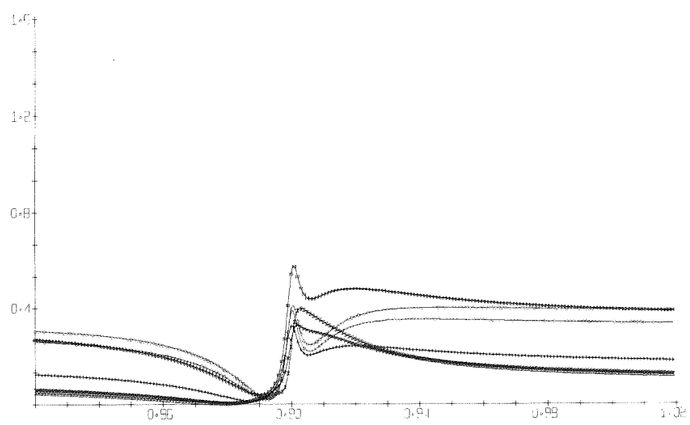
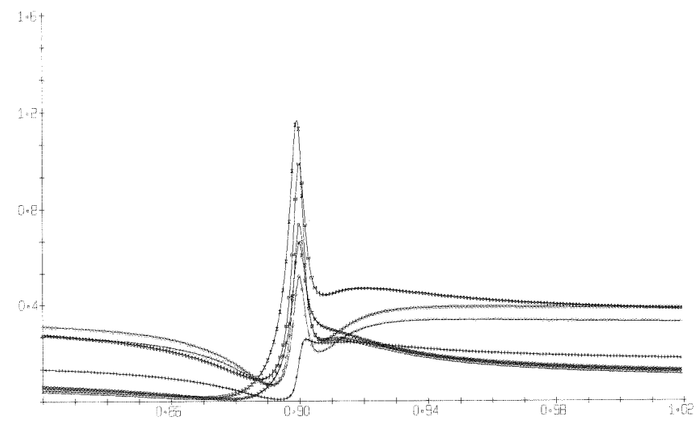
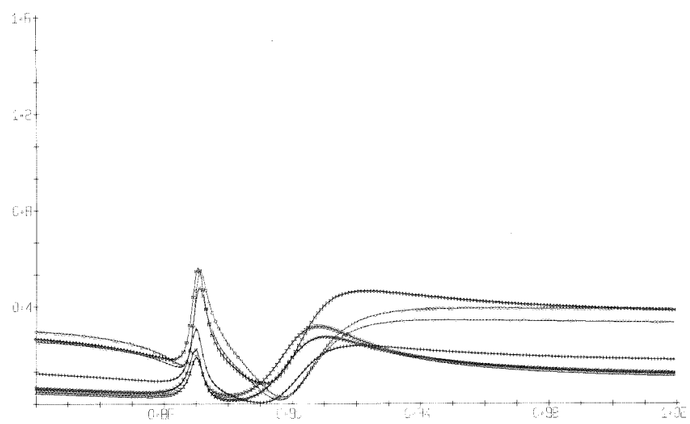
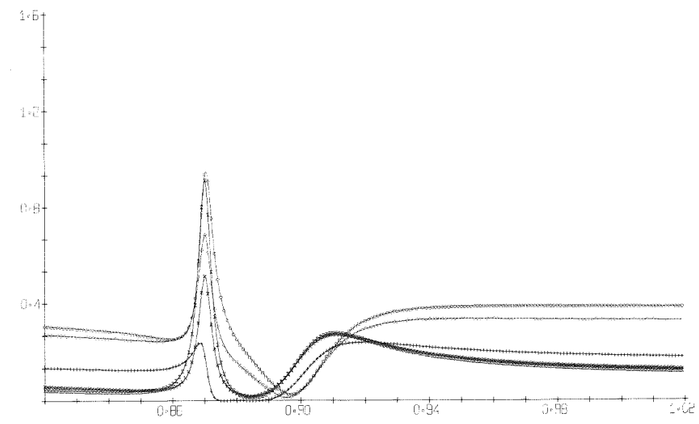
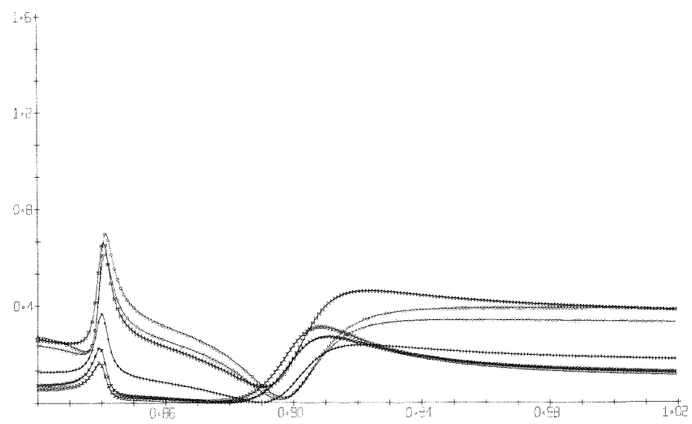
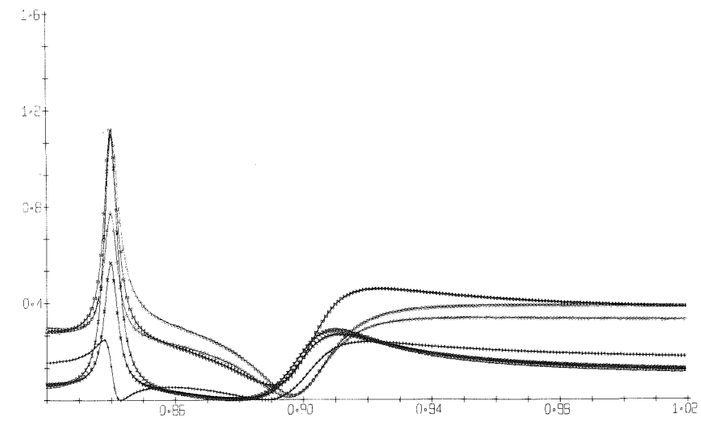

E (MeV)

Fig. 6 $1/2^+$-$1/2^-$ Levels

Coherent Interference Effects

Fig. 7 $1/2^+$-$3/2^+$ Levels

$1/2^+$ Resonance centered at .9 MeV

Differential Cross Sections (barns/steradian)

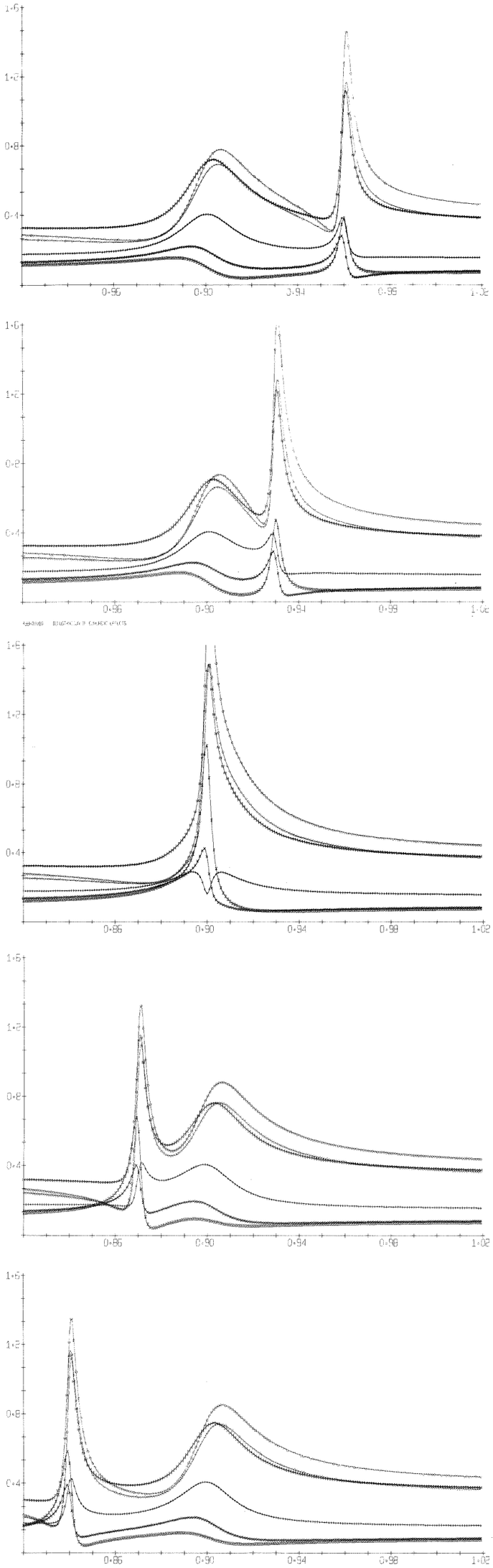

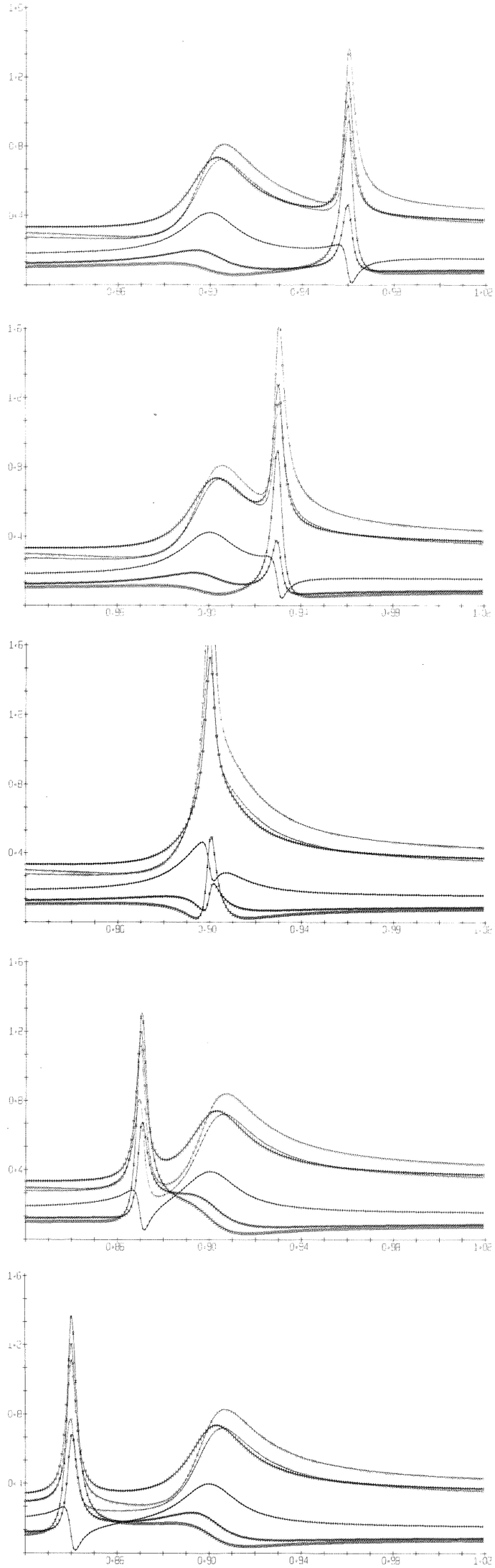

E (MeV)

Fig.8 $1/2^- - 3/2^-$ Levels

Coherent Interference Effects

Fig.9 $1/2^- - 3/2^+$ Levels

$1/2^-$ Resonance centered at .9 MeV

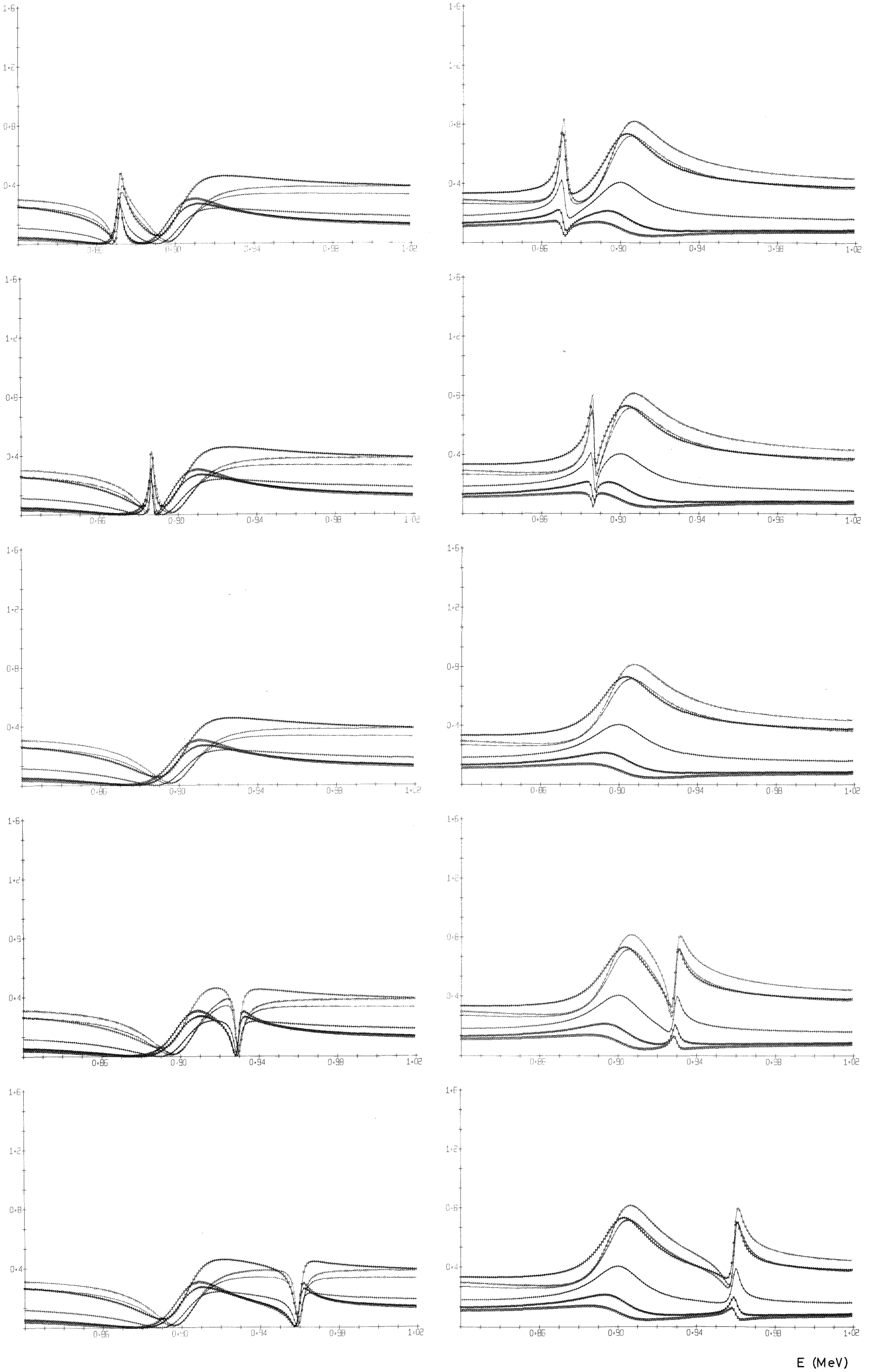

Fig. 10 $1/2^+$ Resonances

Fig. 11 $1/2^-$ Resonances

Multilevel Interference Effects between Levels with Same Spin and Parity

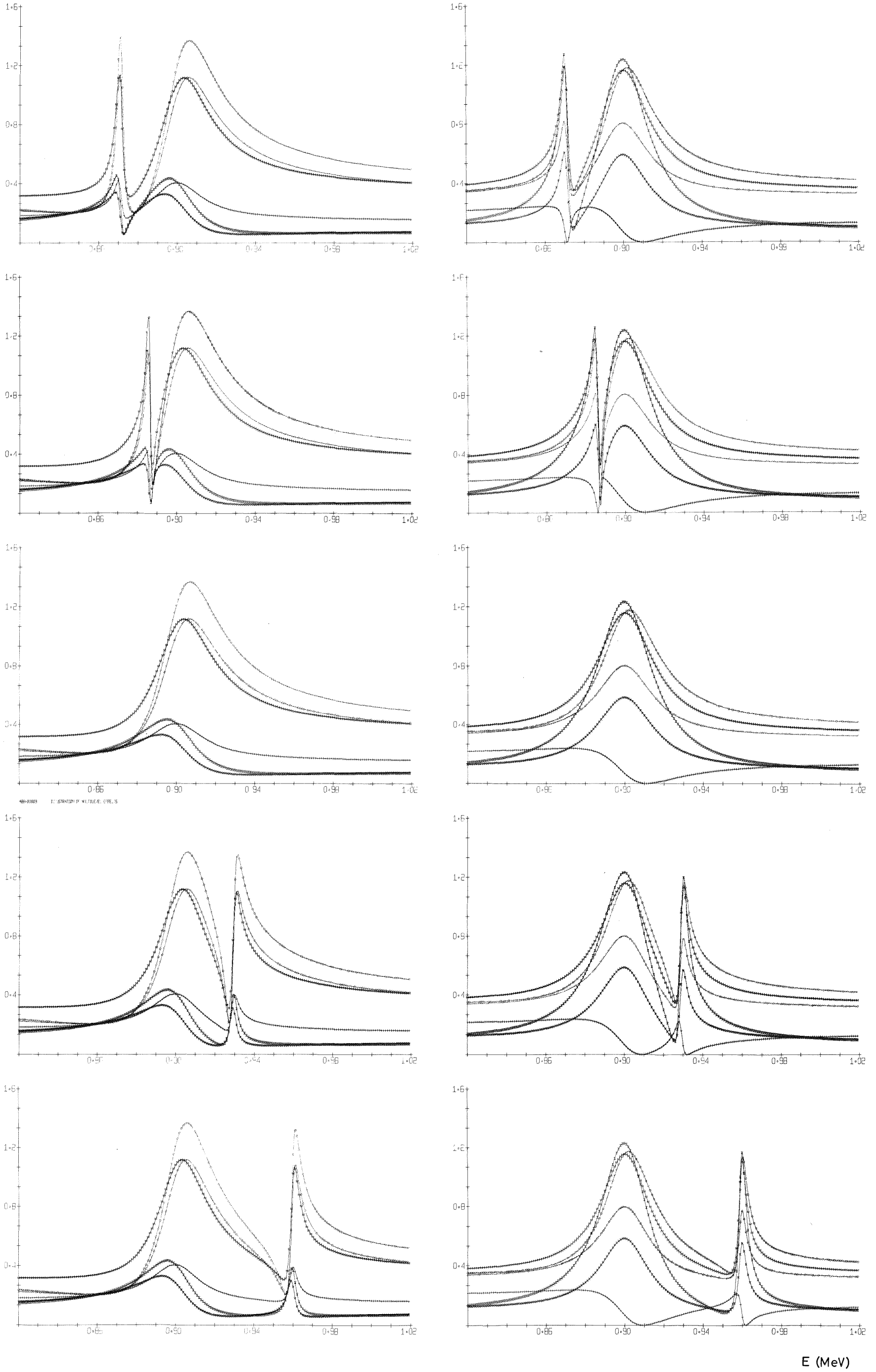

Fig.12 $3/2^-$ Resonances

Fig.13 $3/2^+$ Resonances

Multilevel Interference Effects between Levels with Same Spin and Parity

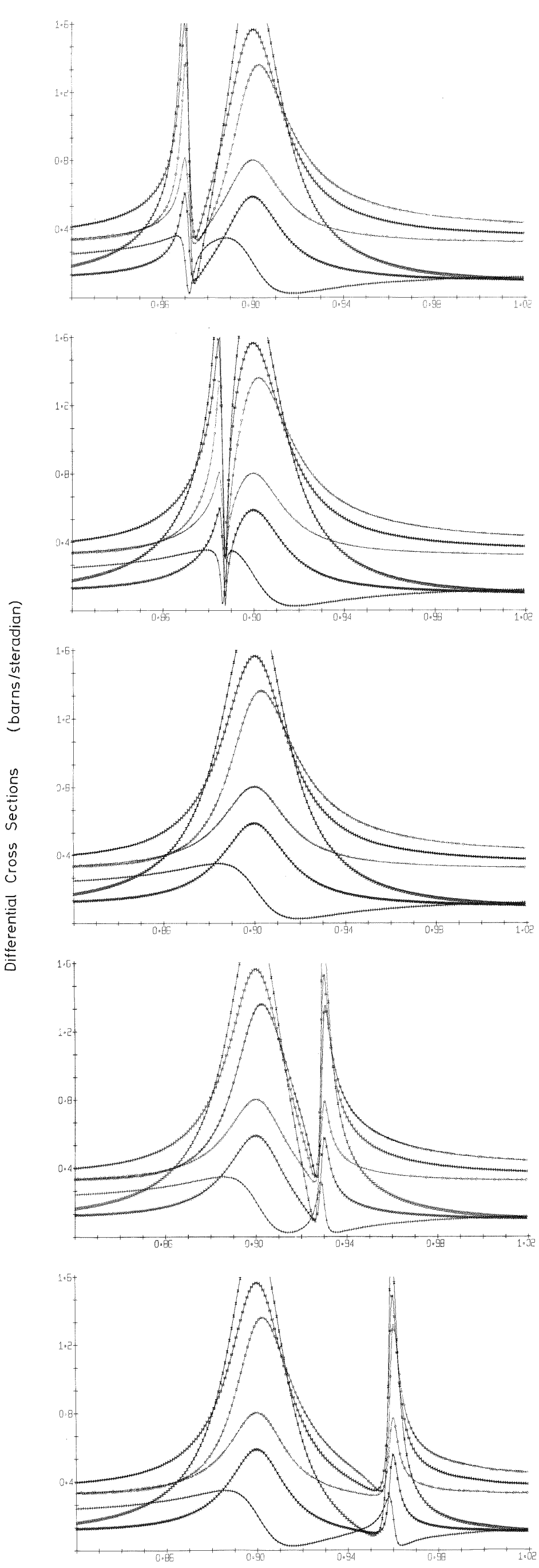

Fig.14 $5/2^{+}$ Resonances
Multilevel Interference

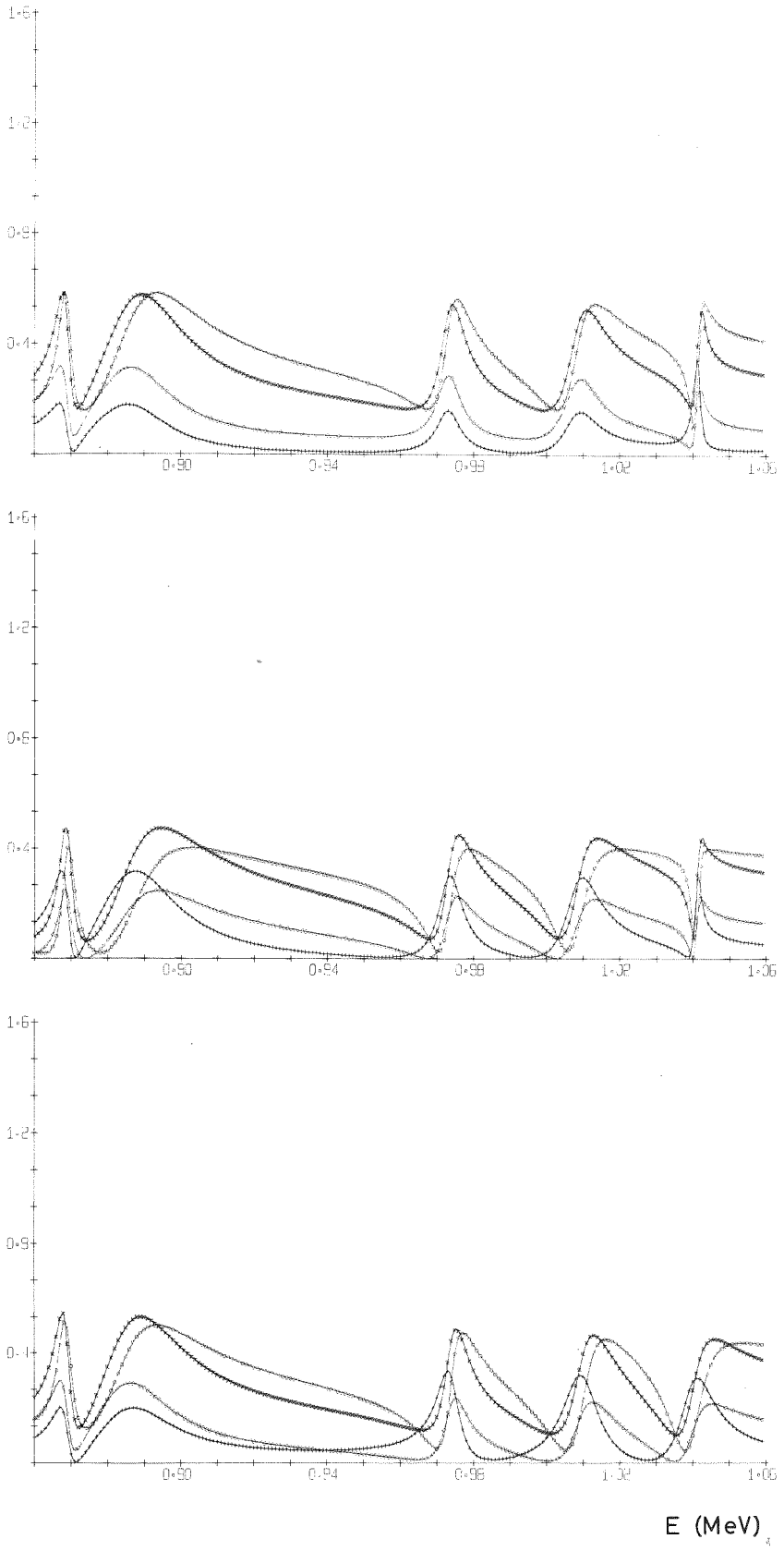

Fig.15 Calcium-40 All p-Waves

Fig.16 Calcium-40 All s-Waves

Fig.17 Calcium-40 Mixed s and p-Waves (see Table I)

Legend for Figures 15 to 17

□ Differential Cross Section (barns/steradian) $45.0^{\circ}_{C.M.}$

◇ Differential Cross Section (barns/steradian) $90.0^{\circ}_{C.M.}$

\+ Differential Cross Section (barns/steradian) $150.0^{\circ}_{C.M.}$

X Total Scattering Cross Section (barns)/ 7.5